Supplemental Material can be found at:
http://www.jbc.org/content/suppl/2009/10/19/M109.056465.DC1.html

THE JOURNAL OF BIOLOGICAL CHEMISTRY VOL. 284, NO. 50, pp. 35154–35164, December 11, 2009
© 2009 by The American Society for Biochemistry and Molecular Biology, Inc. Printed in the U.S.A.

Splicing Factor Arginine/Serine-rich 17A (SFRS17A) Is an A-kinase Anchoring Protein That Targets Protein Kinase A to Splicing Factor Compartments*[S]

Received for publication, August 16, 2009, and in revised form, October 19, 2009 Published, JBC Papers in Press, October 19, 2009, DOI 10.1074/jbc.M109.056465

Elisabeth Jarnæss[‡§1], Anne Jorunn Stokka[‡§], Anne-Katrine Kvissel[¶‖], Bjørn S. Skålhegg[¶‖], Knut Martin Torgersen[‡§], John D. Scott[**], Cathrine R. Carlson[‡2], and Kjetil Taskén[‡§3]

From the [‡]Biotechnology Centre of Oslo, the [§]Centre for Molecular Medicine Norway, Nordic European Molecular Biology Laboratory Partnership, the [¶]Department of Nutrition, and the [‖]Department of Biochemistry, Institute of Basic Medical Sciences, University of Oslo, PB 1125 Blindern, N-0317 Oslo, Norway and the [**]Howard Hughes Medical Institute, Department of Pharmacology, University of Washington School of Medicine, Seattle, Washington 98195

Protein kinase A (PKA) is targeted to distinct subcellular localizations by specific protein kinase A anchoring proteins (AKAPs). AKAPs are divided into subclasses based on their ability to bind type I or type II PKA or both. Dual-specificity AKAPs were recently reported to have an additional PKA binding determinant called the RI specifier region. A bioinformatic search with the consensus RI specifier region identified a novel AKAP, the splicing factor arginine/serine-rich 17A (SFRS17A). Here, we show by a variety of protein interaction assays that SFRS17A binds both type I and type II PKA *in vitro* and inside cells, demonstrating that SFRS17A is a dual-specific AKAP. Moreover, immunofluorescence experiments show that SFRS17A colocalizes with the catalytic subunit of PKA as well as the splicing factor SC35 in splicing factor compartments. Using the *E1A* minigene splicing assay, we found that expression of wild type SFRS17A conferred regulation of *E1A* alternative splicing, whereas the mutant SFRS17A, which is unable to bind PKA, did not. Our data suggest that SFRS17A is an AKAP involved in regulation of pre-mRNA splicing possibly by docking a pool of PKA in splicing factor compartments.

The second messenger cAMP produced in response to G protein-coupled receptor-mediated stimuli controls a variety of physiological responses through protein kinase A (PKA)[4] (reviewed in Ref. 1). In the absence of cAMP, PKA is an inactive tetramer consisting of two regulatory (R) and two catalytic (C) subunits. Upon increased cellular cAMP levels, the enzyme dissociates into an R subunit dimer with bound cAMP and two catalytically active C subunits that phosphorylate nearby substrates (2, 3). PKA subunits are encoded by a family of R and C subunit genes (*RIα*, *RIβ*, *RIIα*, *RIIβ*, *Cα*, *Cβ*, *Cγ*, and *PRKX*). The holoenzymes exhibit distinct cAMP binding affinities and localization inside cells and are classified as type I or type II based on their R subunit composition (4, 5).

PKA is targeted to distinct subcellular loci through interaction with a family of protein kinase A anchoring proteins (AKAPs). AKAPs encompass more than 50 structurally diverse but functionally related proteins that organize and target supramolecular signaling complexes and scaffold signaling pathways. AKAPs serve to organize discrete spatiotemporal regulation of signaling events mediated by PKA (1, 6). Although archetypical AKAPs bind type II PKA, more recent work shows that AKAPs can be defined by their ability to bind type I PKA (RI-specific) (7–9), type II PKA (RII-specific), or both (dual-specific) (10–15). Most AKAPs bind PKA through an amphipathic helix consisting of 14–18 amino acids (16–18) that inserts into a hydrophobic groove formed by the R dimer as evident from resolution of NMR and crystal structures of the complex (19–23). A structure-based substitution approach allowed identification of determinants for RI and RII binding to AKAPs and development of specific high affinity binding sequences (22, 24–26). We recently showed that some dual-specific AKAPs contain an additional binding region, the RI specifier region (RISR), that enhances anchoring of type I PKA (27). This region is detected in a variety of AKAPs, like Ezrin, Merlin, PAP7, D-AKAP1 and D-AKAP2, and provides a mechanism for multisite binding to the RI subunit, thus enhancing the affinity and specificity of type I PKA binding to AKAPs (27). Furthermore, AKAPs, such as pericentrin (28) and α4 integrins (9), contain neither the amphipathic helix nor RISR-like sequences but display distinct, non-classical types of PKA binding sites.

Upon activation of the PKA holoenzyme, a part of the C subunit pool enters the nucleus, where it is involved in regulation of transcription and splicing (29). Introns are removed from pre-mRNAs by the spliceosome, a massive complex that

* This work was supported by grants from the Norwegian Functional Genomics Program, the Research Council of Norway, the Norwegian Cancer Society, Novo Nordic Foundation, and European Union Grant 037189 (theracAMP). This work was also supported, in part by National Institutes of Health Grant DK54441 (to J. D. S.).

[S] The on-line version of this article (available at http://www.jbc.org) contains supplemental Table 1 and Figs. S1 and S2.

[1] A fellow of The University of Oslo.

[2] Present address: Institute for Experimental Medical Research, Ullevaal University Hospital, Kirkeveien 166, N-0407 Oslo, Norway.

[3] To whom correspondence should be addressed: The Biotechnology Centre of Oslo, University of Oslo, P.O. Box 1125, Blindern, N-0317 Oslo, Norway. Tel.: 47-22840505; Fax: 47-22840506; E-mail: kjetil.tasken@biotek.uio.no.

[4] The abbreviations used are: PKA, protein kinase A; 8-AHA-cAMP, 8-(6-aminohexyl)aminoadenosine-3′,5′-cyclic monophosphorothioate; Rp-8-AHA-cAMP, 8-(6-aminohexyl)aminoadenosine-3′,5′-cyclic monophosphorothioate, Rp-isomer, immobilized on agarose; AKAP, A-kinase anchoring protein; RISR, RI specifier region; GFP, green fluorescent protein; SFC, splicing factor compartment; GST, glutathione S-transferase; Mops, 4-morpholinepropanesulfonic acid; BSA, bovine serum albumin; TBS, Tris-buffered saline; SPR, surface plasmon resonance; SR, serine/arginine.

Downloaded from www.jbc.org at University of Washington Health Sciences Libraries, on January 7, 2010

Supplemental Material can be found at:
http://www.jbc.org/content/suppl/2009/10/19/M109.056465.DC1.html

consists of five small nuclear ribonucleoprotein particles, U1, U2, U4, U5 and U6, associated with a large number of proteins. The spliceosome assembles in a stepwise manner via multiple RNA-RNA, RNA-protein, and protein-protein interactions. Components of the splicing machinery are recruited to sites of transcription from splicing factor compartments (SFCs), which are dynamic structures located within the nucleoplasm. Many pre-mRNA splicing factors, including small nuclear ribonucleoproteins and SR proteins, such as ASF/SF2 and SC35, localize to SFCs (30–32). In addition, SFCs contain several kinases and phosphatases that can modify the phosphorylation status of components of the splicing machinery. It has been suggested that SFCs are storage/assembly/modification sites for the splicing machinery whose main function is to regulate the pool of factors available to the transcription and pre-mRNA processing machinery (33).

SR proteins regulate both alternative and constitutive splicing. In addition to the serine/arginine-rich domain, SR proteins also contain an RNA recognition motif (34, 35). Previous studies have suggested that SFRS17A is an alternative splicing factor and an SR-related splicing protein that interacts with the classical SR protein ASF/SF2 and the SR-related factor ZNF265 (36). SFRS17A is ubiquitously transcribed and gives rise to two alternatively spliced isoforms of 695 and 385 amino acids (37). Whereas the long form involved in splicing has almost 30% arginine and serine in the last 300 amino acids, typical for SR proteins (37), the short form is suggested to be a target for degradation by nonsense-mediated mRNA decay and has, as of yet, no function assigned (38). SFRS17A was originally reported as the pseudoautosomal or X inactivation escape gene 7 (XE7) and as B-lymphocyte antigen precursor.

Here, we demonstrate that SFRS17A is a dual-specific AKAP that binds type I and type II PKA with high affinity and colocalizes with the PKA C subunit in nuclear speckles. Furthermore, we demonstrate that SFRS17A significantly influences the splicing pattern of the *E1A* minigene, whereas SFRS17A mutated in the PKA binding domain does not.

EXPERIMENTAL PROCEDURES

Cell Cultures—Jurkat cells expressing the SV40 large T-antigen (Jurkat TAg) and U-2OS cells were cultured in RPMI 1640 (Invitrogen) supplemented with 10% fetal bovine serum, 100 units/ml penicillin, 1 mM pyruvate, and 1× nonessential amino acids (complete medium). HEK293 and HEK293T cells were grown in complete Dulbecco's modified Eagle's medium. All cells were cultured at 37 °C with 5% CO_2.

Constructs—Full-length SFRS17A was inserted into pFLAG-CMV-5a and pEGFP-N3. A truncated SFRS17A (amino acids 353–533) was inserted into pGEX-5X1 to generate a glutathione *S*-tranferase (GST)-fused construct. Substitutions L438P, L439P, K445P, and K446P were introduced in the R-binding domain of SFRS17A-FLAG to abolish binding (SFRS17A mut-FLAG) by mutagenesis (QuickChange, Stratagene) using two primer sets: SFRS17A(L438P/L439P) sense (5′-tgcgcgagcggccgccgagcatcctgct-3′) and antisense (5′-agcaggatgctcggcggccgctcgcgca-3′) and SFRS17A(K445P/K446P) sense (5′-tgagcatcctgctgagcccgccgccggacgacagccaca-3′) and antisense (5′-tgtggctgtcgtccggcggcgggctcagcaggatgctca-3′). All constructs were confirmed by sequencing.

Antibodies—Polyclonal antibodies to SFRS17A were generated by Covance by inoculating New Zealand White rabbits with a keyhole limpet hemocyanin-tagged peptide, CNREPSKGRGRATGDGL, corresponding to amino acids 579–595 of SFRS17A (AAA61304), using their standard protocol including a total of five peptide injections over a period of 118 days. Antiserum was affinity-purified by immobilizing immunizing peptide on Affi-Gel® 10 (Bio-Rad), followed by column chromatography and elution with IgG elution buffer (Pierce). Purified antibody fractions were immediately adjusted to physiological pH by the addition of 1 M phosphate buffer (pH 7.0) before the antibodies were extensively dialyzed against TBS buffer. For immunoblotting the following antibodies were used: monoclonal mouse anti-AKAP 149 (1:500), mouse anti-GFP (1:1000), mouse anti-RIα (1:250), and mouse anti-RIIα (1:500) from BD Biosciences and polyclonal anti-FLAG M2 (1:1000) from Cell Signaling. Mouse monoclonal anti-PKAα catalytic subunit (1:500) was from Santa Cruz Biotechnology, Inc. (Santa Cruz, CA), whereas mouse monoclonal anti-T7 (1:1000) was from Novagen.

Protein Expression and Purification—Bovine RIα and human RIIα proteins were expressed in *Escherichia coli* BL21 and *E. coli* Rosetta, respectively, using 0.1–1.0 mM isopropyl-β-D-thiogalactopyranoside induction at room temperature (4 h) and purified on Rp-8-AHA-cAMP-agarose beads (BioLog) as described previously (39). GST-SFRS17A-(353–533) was expressed in *E. coli* Rosetta cells, induced using 0.1 mM isopropyl-β-D-thiogalactopyranoside at room temperature (4 h), and purified on glutathione-Sepharose beads (Sigma). The purified recombinant R proteins were dialyzed extensively against 20 mM Mops (pH 7) and 150 mM NaCl, and SFRS17A fused to GST was dialyzed against 50 mM Tris-HCl (pH 8) and 150 mM NaCl. Protein concentrations were determined using the Bradford protein assay and SDS-PAGE (10% gels) using BSA as a standard.

Peptide Synthesis—Peptides used for Surface Plasmon Resonance studies (RISR, ESKRRQEEAEQRK; RISR(Q6P/R12P), ESKRPQEEAEPRK) were synthesized on an Intavis MultiPep robot (Intavis Bioanalytical Instruments AG) and verified by high performance liquid chromatography. Concentrations of the peptides were determined by amino acid analysis using an amino acid analyzer from Applied Biosystems. Immunizing peptide used for antibody production (SFRS17A-(579–595), CNREPSKGRGRATGDGL) and the negative control peptide used for characterization of the SFRS17A antibody (SFRS17A-(167–176), KESGSEKPSEDVLVK) were produced by Novagen.

Autospot Peptide Array—Peptide spots were synthesized with Fmoc (*N*-(9-fluorenyl)methoxycarbonyl)-protection chemistry on cellulose membranes using a Multipep automated peptide synthesizer (Intavis Bioanalytical Instruments AG) as described (40).

Presence of SFRS17A in Cell Lines—RNA was isolated from different cell lines using RNeasy (Qiagen). First strand cDNA was synthesized using the iScript cDNA kit (Bio-Rad). PCR was performed using the primers SFRS17A forward (5′-GAGCCAAGGCTGTGAAGCTA) and SFRS17A reverse (5′-CGACAGGAGCTCTGAACCTC) and a program involving 95 °C

Downloaded from www.jbc.org at University of Washington Health Sciences Libraries, on January 7, 2010

Supplemental Material can be found at:
http://www.jbc.org/content/suppl/2009/10/19/M109.056465.DC1.html

for 5 min, 30 cycles of 94 °C for 1 min, 56 °C for 45 s, 72 °C for 45 s, and finally 72 °C for 10 min, resulting in a PCR product of 445 bp. PCR products were analyzed on a 2% agarose gel stained with ethidium bromide.

Cell Fractionation—Subcellular protein fractionation from cellular components in HEK293T cells was performed using the Qproteome Cell Compartment kit according to the manufacturer's instructions (Qiagen).

Immunoprecipitation—HEK293T cells at 50–80% confluence were transfected with 5–10 μg of plasmid DNA (SFRS17A-GFP, empty vector GFP, SFRS17A-FLAG,SFRS17A(L438P/L439P/K445P/K446P)-FLAG, or empty vector FLAG) per 10-cm dish using Lipofectamine™ (Invitrogen) or FuGENE® 6 (Roche Applied Science). Cells were lysed 24 h after transfection in lysis buffer (50 mM Tris-HCl (pH 7.4), 400 mM NaCl, 1 mM phenylmethylsulfonyl fluoride, 1 mM Na_3VO_4, 0.5% Triton X-100) with protease inhibitors (Complete Mini EDTA-free tablets; Roche Applied Science). Immunoprecipitations were carried out using antibodies against PKA-RIIα and/or PKA-RIα (BD Transduction Laboratories). Immunocomplexes were washed three times in lysis buffer before being subjected to SDS-PAGE followed by immunoblotting with the indicated antibodies.

R Overlay—R overlays were conducted as described (16), using ^{32}P-labeled recombinant murine RIIα (41) or recombinant bovine RIα (A98S), substituted to allow autophosphorylation (42). Briefly described, the membrane with immobilized peptide or protein was blocked in Blotto (5% (w/v) nonfat dry milk and 0.1% BSA in TBS. Purified recombinant R (4 μg) was radiolabeled with purified C subunit of PKA (0.02 μg/μl) and [γ-^{32}P]ATP (1.4 μCi/μl) in 50 mM Mops (pH 6.8), 50 mM NaCl, 2 mM $MgCl_2$, and 1 mM dithiothreitol and separated from free [^{32}P]ATP by gel filtration (G-50 Sepharose). Specific activity was quantified by liquid

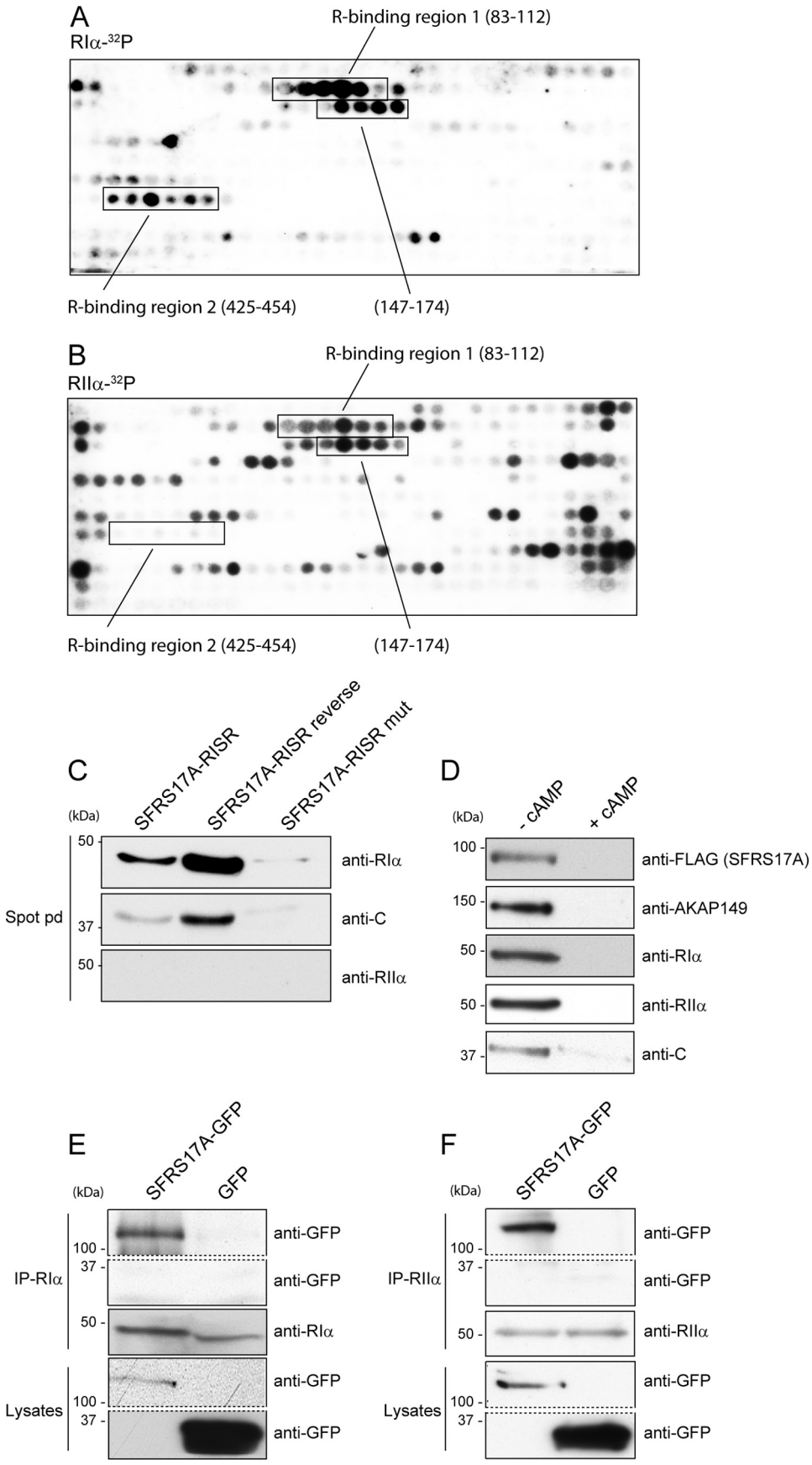

Downloaded from www.jbc.org at University of Washington Health Sciences Libraries, on January 7, 2010

Supplemental Material can be found at:
http://www.jbc.org/content/suppl/2009/10/19/M109.056465.DC1.html

scintillation counting (1600TR Tri-Carb, Packard Instrument Co.). All overlays were incubated overnight at room temperature using 1×10^6 cpm/ml TBS, 0.01% Tween 20 (TBS-T). For competition assays, soluble peptide was added to the radiolabeled RIIα and incubated for 2 h before adding the membrane. The membrane was washed five times in TBS-T, and the signal was detected by autoradiography.

Solid Phase Pull-down—Lysate from 40×10^6 Jurkat TAg cells was incubated overnight at 4 °C with SFRS17A-RISR (RKERELRERLLSILLSKKPD) or SFRS17A-RISR mut (RKERELRERLLSILLSPPPD) peptide synthesized in triplicates on cellulose membrane. The membranes were subsequently washed twice (20 min) in lysis buffer (50 mM Hepes (pH 7.4), 10 mM $NaPP_i$, 0.1% Triton X-100, 50 mM NaF, 100 mM NaCl, 5 mM EDTA, 1 mM phenylmethylsulfonyl fluoride, 1 mM Na_3VO_4) with protease inhibitors (Complete Mini EDTA-free tablets, Roche Applied Science) and twice in high salt lysis buffer (1 M NaCl). Bound PKA was eluted by boiling in SDS-PAGE sample buffer and analyzed by Western blotting with the indicated antibodies.

cAMP Affinity Chromatography—Transfected HEK293T cells (10-cm dish) were lysed in radioimmune precipitation buffer (50 mM Tris-HCl (pH 7.8), 500 mM NaCl, 1% Nonidet P-40, 0.5% deoxycholate, 0.1% SDS) and incubated overnight at 4 °C with Rp-8-AHA-cAMP-agarose bead slurry in the presence or absence of 75 mM cAMP. Beads were subsequently washed once in high salt buffer (10 mM Hepes, pH 7.4, 1.5 mM $MgCl_2$, 10 mM KCl, 0.5 M NaCl, 0.1% Nonidet P-40, 1 mM dithiothreitol) with protease inhibitors (Complete Mini EDTA-free tablets, Roche Applied Science) and twice in low salt buffer (10 mM Hepes, pH 7.4, 1.5 mM $MgCl_2$, 10 mM KCl, 0.1% Nonidet P-40, 1 mM dithiothreitol) with protease inhibitors. Proteins bound to the beads were eluted with 75 mM cAMP, pH 7.0, for 1 h at room temperature before they were subjected to SDS-PAGE and immunoblotting with indicated antibodies.

Surface Plasmon Resonance—The binding studies between PKA-R and SFRS17A were performed on a BIAcore T100 instrument (BIAcore Life Sciences/GE Healthcare Europe). CM5 chips (Biacore), coated with 8-AHA-cAMP (BioLog), were used to capture cAMP-free bovine RIα, and human RIIα subunits at a flow rate of 5 μl/min (surface immobilization level of 100–230 response units for each subunit) as described previously (39) in running buffers at pH 7.4 (for RI, 10 mM Hepes, 150 mM NaCl, 50 μM EDTA, 0.5 mM ATP, 10 mM $MgCl_2$, and 0.1% surfactant P20; for RII, 10 mM Hepes, 150 mM NaCl, 50 μM EDTA, and 0.1% surfactant P20). All subsequent interaction studies were performed in running buffers at pH 8 (for RI, 50 mM Tris, 150 mM NaCl, 50 μM EDTA, 0.5 mM ATP, 10 mM $MgCl_2$, and 0.1% surfactant P20; for RII, 50 mM Tris, 150 mM NaCl, 50 μM EDTA, and 0.1% surfactant P20) at 25 °C. The fusion protein GST-SFRS17A-(353–533) was injected at a flow rate of 30 μl/min in a series of dilutions (from 62.5 to 2.0 nM; for 90 s) to determine the affinity of the interaction. After injection, the dissociation phase was monitored for 300 s. Nonspecific binding was subtracted using blank runs performed on a surface immobilized with 8-AHA-cAMP with no R-subunit captured. Competition experiments were performed on immobilized bovine PKA-RIα or human PKA-RIIα subunits. 50 nM GST-SFRS17A-(353–533) was injected in the presence or absence of 10 μM RISR or RISR(Q6P/R12P) at a flow rate of 30 μl/min for 90 s, and the binding level to the R subunit was analyzed. RISR peptide was also injected in the absence of AKAP. Kinetic analysis was performed using the BIAcore T100 evaluation software.

E1A Splicing Assay—E1A splicing assays were performed as described (29). Briefly described, U-2OS cells grown in 6-well dishes were co-transfected with 0.5 μg of the splicing reporter minigene *E1A* and 1.5 μg of either Cα, SFRS17A, SFRS17A(L438P/L439P/K445P/K445P), ASF/SF2, or empty pFLAG-CMV-5a plasmid using FuGENE® 6 (Roche Applied Science). Twenty hours after transfection, RNA was isolated using RNeasy (Qiagen). First strand cDNA was synthesized using the iScript cDNA kit (Bio-Rad). PCR was performed using primers *E1A* forward (5′-GTTTTCTCCTCCGAGCCGCTCCGA) and *E1A* reverse (5′-CTCAGGCTCAGGTTCAGACACAGG) and a program involving 95 °C for 5 min, 25 cycles of 94 °C for 30 s, 62 °C for 20 s, 72 °C for 40 s, and finally 72 °C for 10 min. PCR products were separated on a 1.5% agarose gel stained with Gelstar® (Cambrex). Protein extracts were prepared from the same samples to study expression levels of transfected plasmids.

Immunofluorescence Analysis—For immunofluorescence analysis, HEK293T cells were grown on coverslips coated with collagen and fibronectin (both from Sigma) for 48 h. At room temperature, cells were fixed with 3% paraformaldehyde in phosphate-buffered saline (PBS) for 15 min, permeabilized with 0.1% Nonidet P-40, PBS for 5 min, and then blocked for 30 min with 2% BSA, 0.01% Tween 20, PBS (PBST-BSA). The primary antibodies anti-rabbit SFRS17A (1:100; custom made), anti-mouse SC35 (1:100; Sigma), or anti-mouse PKAα catalytic subunit (1:100; Santa Cruz Biotechnology, Inc.) in PBST-BSA were added for 30 min. Cells were then incubated with fluorochrome-conjugated secondary antibodies (Alexa Fluor 488 goat anti-mouse IgG, Alexa Fluor 488 goat anti-rabbit IgG, Alexa Fluor 546 goat anti-rabbit IgG, and Alexa Fluor 546 goat anti-mouse IgG (1:500); Molecular Probes) in PBST-BSA for 30 min before being mounted with glass coverslips using fluorescent mounting medium (DakoCytomation). Confocal microscopy was performed with a Zeiss LSM 510 META confocal microscope with a Plan-Apochromat 63 × 1.4 oil differential interference contrast objective lens, using laser excitation at 488 and 546 nm. Pictures were obtained using sequential scanning, and

FIGURE 1. **Identification of SFRS17A as an AKAP.** *A* and *B*, the full-length human SFRS17A sequence was spotted as overlapping 20-mer peptides with 2-amino acid shifts on cellulose membranes and subjected to overlay using radiolabeled RIα (*A*) or RIIα (*B*). Binding was detected by autoradiography. *C*, SFRS17A-RISR solid phase pull-down (*pd*). 20-mer SFRS17A-RISR peptides synthesized in triplicate on membrane were incubated in Jurkat tag cell lysate overnight, and immobilized proteins were eluted and subjected to SDS-PAGE and immunoblotting. *D*, FLAG-tagged SFRS17A (full-length) was tested for interaction with PKA by cAMP pull-down. The presence of cAMP throughout the experiment was used as a negative control. *E and F*, co-immunoprecipitation (*IP*) of the GFP-fused SFRS17A (full-length) protein with PKA-RIα (*E*) or PKA-RIIα (*F*), as detected by anti-GFP immunoblotting. *A–C* are representative of four independent experiments. *D–F* represent three independent experiments.

Downloaded from www.jbc.org at University of Washington Health Sciences Libraries, on January 7, 2010

Supplemental Material can be found at:
http://www.jbc.org/content/suppl/2009/10/19/M109.056465.DC1.html

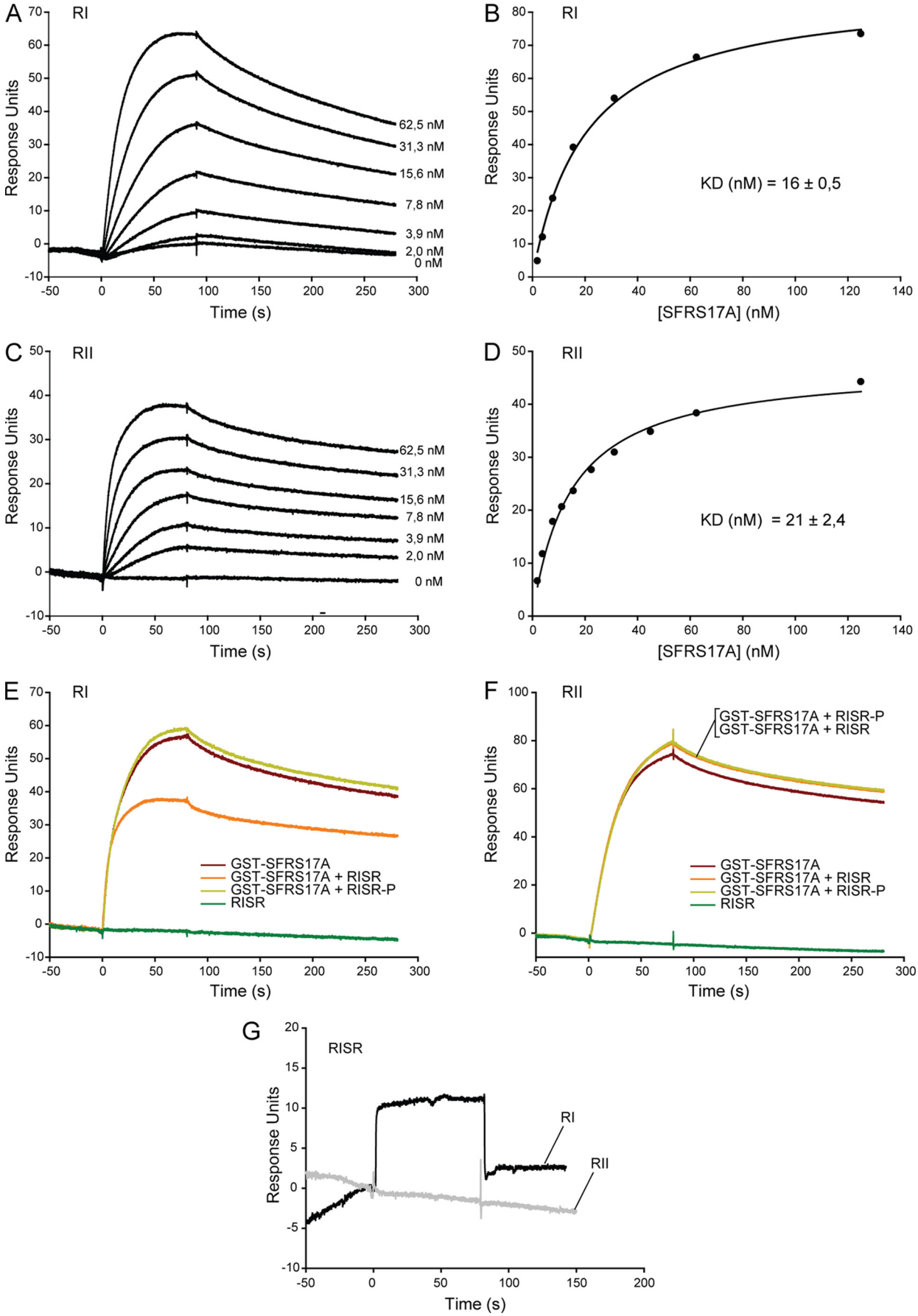

Downloaded from www.jbc.org at University of Washington Health Sciences Libraries, on January 7, 2010

Supplemental Material can be found at:
http://www.jbc.org/content/suppl/2009/10/19/M109.056465.DC1.html

the exposure settings and gain of laser were kept the same for each condition.

Statistical Analysis—Data are presented as mean ± S.E. Paired statistical analyses were performed using Student's *t* test. The two-sided *p* values were considered statistically significant at $p < 0.05$.

RESULTS

Identification of SFRS17A as an AKAP—We previously reported that dual-specificity AKAPs contain an additional binding region, RISR, increasing the affinity and specificity of type I PKA binding (27). A bioinformatics search in the International Protein Index data base, using a RISR consensus sequence ($LX_3E_2X_6E$) as probe, identified SFRS17A as one of nine proteins with a putative RISR (supplemental Table 1). We explored the possibility that SFRS17A could be a novel AKAP. To analyze SFRS17A binding to PKA, a family of 339 overlapping 20-mer peptides (offset by two residues) were synthesized on peptide array and subjected to overlay with radiolabeled RI and RII. RI bound three different regions in SFRS17A: residues 83–112 (VENKSLVKSFLACLDGKTIKLSGFSDILKV, R-binding region 1), residues 147–174 (DTIHLEGLPCKWFALKESGSEKPSEDVLV), and residues 425–454 (LGLQRKERELRERLLSILLSKKPDDSHTHD, R-binding region 2) (Fig. 1*A*). The region covering residues 147–174, which did not contain any RISR or amphipathic helix structure but rather two helix-breaking prolines, did not appear to bind in subsequent analyses and was consequently excluded as a putative RI/RII binding site. The most N-terminal region (R-binding region 1) bound RII as well as RI (Fig. 1*B*) and, by modeling in α-helical configuration, appeared to contain an amphipathic helix. However, no RISR sequence was identified in this region. In contrast, the most C-terminal region (R-binding region 2) contained a putative RISR encompassing amino acids 426–437 (GLQRKERELRER), to which little RII binding was observed. Furthermore, R-binding region 2 was, by more detailed mapping using a combination of overlapping peptides offset by one residue and peptides with N- and C-terminal truncations, found to contain a partially overlapping sequence in residues 433–446 that could also be modeled as an amphipathic helix (supplemental Fig. S1, *A–C*).

R-binding region 2 in SFRS17A with the RISR sequence was next utilized in a solid phase pull-down assay, where immobilized 20-mer SFRS17A-RISR or negative control peptide, SFRS17A-RISR mut, synthesized on membranes was incubated in a Jurkat TAg cell lysate. Substitutions in the control peptide were made based on the results obtained from a two-dimensional peptide array performed with the SFRS17A-RISR sequence (supplemental Fig. S2*A*). Bound proteins were eluted with SDS loading buffer, and the presence of PKA subunits was assessed by immunoblotting using specific antibodies. As shown in Fig. 1*C*, both PKA-RIα and PKA C subunits but not PKA-RIIα were pulled down by the SFRS17A-RISR peptide. Interestingly, PKA-RIα and PKA C also bound SFRS17A-RISR in the reverse orientation. Having established that SFRS17A binds PKA *in vitro*, the SFRS17A-PKA interaction was then studied *in situ* with coprecipitation experiments. Full-length FLAG-tagged SFRS17A containing R binding regions 1 and 2 was expressed in HEK293T cells and cell lysate subjected to affinity chromatography on Rp-8-AHA-cAMP-agarose in the absence and presence of excess free cAMP, which competes binding. Rp-8-AHA-cAMP is a PKA antagonist that does not dissociate the C subunit from the PKA holoenzyme. As expected, RI, RII, and C were in the eluate from the column when conducting the chromatography in the absence, but not in the presence, of excess cAMP (Fig. 1*D*). Furthermore, both FLAG-tagged SFRS17A and endogenous AKAP149 as a positive control were copurified with PKA on the Rp-8-AHA-cAMP-agarose (Fig. 1*D*). Immunoprecipitation of both RI (Fig. 1*E*) and RII (Fig. 1*F*) coprecipitated full-length SFRS17A-GFP. In contrast, GFP expressed alone was not detected in the control immune complexes (Fig. 1, *E* and *F*).

Kinetics of the SFRS17A-PKA Interaction—To characterize the kinetics of the SFRS17A-PKA interaction, we next used surface plasmon resonance (SPR) analysis (Fig. 2). In this experiment, cAMP-free bovine RIα (Fig. 2*A*) or human RIIα (Fig. 2*C*) were immobilized onto the surface of a CM5 sensor chip coated with 8-AHA-cAMP, and a GST-tagged fragment of SFRS17A, encompassing amino acids 353–533, was injected over the surfaces. As evident from the sensograms from chips with RI or RII immobilized (Fig. 2, *A* and *C*), as well as from the steady state binding isotherms (Fig. 2, *B* and *D*), SFRS17A-(353–533) demonstrated a concentration-dependent binding with nanomolar affinity for both RI ($K_D = 16 \pm 0.5$ nM) and RII ($K_D = 21 \pm 2.4$ nM). Binding of GST-SFRS17A-(353–533) to RI was partially competed with 10 μM RISR peptide (27) (Fig. 2*E*), whereas no effect was seen on the binding to RII in the presence of peptide (Fig. 2*F*). This confirms the results obtained in an earlier study (27) of RISR being an RI specifier and indicates that the RISR identified inside R binding region 2 in SFRS17A contributes to RI but not to RII binding. This is also supported by injecting the RISR alone over surfaces with RI or RII bound (Fig. 2*G*, enhanced and with a different scale to visualize binding of the smaller mass of the RISR as compared with SFRS17A). In contrast, no effect was seen on either RI or RII binding with the proline-substituted RISR(Q6P/R12P) negative control peptide.

FIGURE 2. **Analysis of the kinetics of the SFRS17A-PKA interaction.** *A* and *C*, SPR studies of the GST-SFRS17A-(353–533) binding to immobilized bovine PKA-RI (*A*) or human PKA-RII (*C*) on a sensor chip coated with 8-AHA-cAMP. GST-SFRS17A-(353–533) at the concentrations indicated was injected for 90 s, and the dissociation phase was monitored for 300 s. The *graphs* are representative of four independent experiments performed on different sensor surfaces. *B* and *D*, steady state binding of the increasing GST-SFRS17A-(353–533) concentrations obtained from *A* or *C*, respectively. The affinity constant (K_D) was derived, assuming a 1:1 Langmuir binding model using a global fit analyses algorithm provided by the BIAcore T100 evaluation software. *E–G*, qualitative surface competition experiments with the RISR peptide. 50 nM GST-SFRS17A-(353–533) was injected on a chip with captured bovine PKA-RI (*E*) or human PKA-RII (*F*) in the presence or absence of 10 μM RISR or RISR(Q6P/R12P) peptide. The RISR peptide was also injected without GST-SFRS17A present (*traces* in *E* and *F* as well as a separate experiment in *G* with enhanced sensitivity and different scale to visualize binding of the smaller mass represented by RISR). The *graphs* show one representative experiment of three (or four) independent experiments performed on different chips.

Downloaded from www.jbc.org at University of Washington Health Sciences Libraries, on January 7, 2010

Supplemental Material can be found at:
http://www.jbc.org/content/suppl/2009/10/19/M109.056465.DC1.html

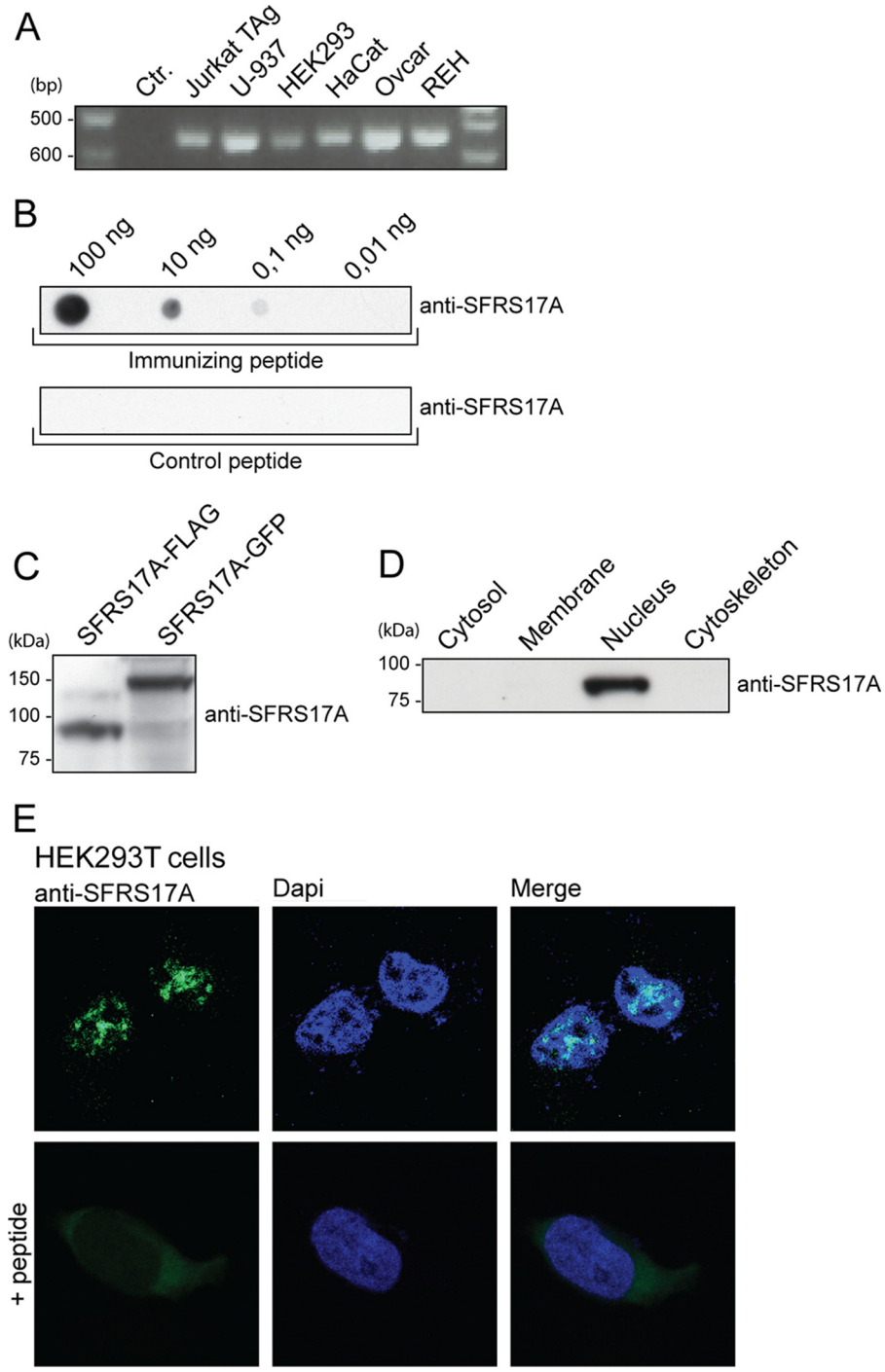

FIGURE 3. **Expression and subcellular localization of SFRS17A.** *A*, SFRS17A expression was detected by reverse transcription-PCR in all cell lines tested. *B*, different amounts of the immunizing peptide used to inoculate New Zealand White rabbits or a negative control peptide (*Ctr.*) was spotted on cellulose paper and detected by anti-SFRS17A immunoblotting. *C*, HEK293T cells were transfected with SFRS17A-FLAG or SFRS17A-GFP and lysed in radioimmune precipitation lysis buffer prior to anti-SFRS17A immunoblotting (lysate from 0.5×10^6 cells loaded into each well). *D*, HEK293T cells (5×10^6 cells) were subjected to subcellular fractionation using the Qproteome cell fractionation kit (Qiagen), and 30 μl of each fraction was subjected to SDS-PAGE and immunoblotting. Endogenous SFRS17A was detected with the use of anti-SFRS17A. *E*, anti-SFRS17A was used for endogenous localization of SFRS17A. Immunizing peptide competes out staining of SFRS17A. *A*, *C*, and *D* are representative of three independent experiments.

Expression and Subcellular Localization of SFRS17A—Examination of SFRS17A expression by reverse transcription-PCR demonstrated that the SFRS17A mRNA was present in all cell lines tested (Fig. 3*A*). For immunolocalization studies of the endogenous SFRS17A protein, antibodies were generated by peptide immunization of rabbits. The specificity of the antibodies was first evaluated by immunoblotting against different amounts of spotted immunizing peptide. The crude SFRS17A antibodies showed high specificity to the peptide antigen (Fig. 3*B*, *top*) without any reactivity toward a negative control peptide derived from another region of SFRS17A (*bottom*). The specificity of the purified anti-SFRS17A was further evaluated by immunoblotting of cell lysates from HEK293T cells transfected with FLAG- or GFP-tagged SFRS17A (Fig. 3*C*). The polyclonal SFRS17A antibodies detected proteins with molecular masses corresponding to the predicted masses for the FLAG- and GFP-tagged SFRS17A, respectively. Next, HEK293T cells were fractionated into nuclei, cytoplasm, membrane, and cytoskeletal fractions and examined for the presence of endogenous SFRS17A by immunoblotting. Endogenous SFRS17A was only observed in the nuclear fraction (Fig. 3*D*). The subcellular distribution of endogenous SFRS17A in HEK293T cells was further examined by immunofluoresence, which demonstrated specific staining of spots in the nucleus (Fig. 3*E*, *top*), consistent with previous observations (36). The specificity of the staining was confirmed by incubation with the immunizing peptide, which resulted in loss of staining (Fig. 3*E*, *bottom*).

SFRS17A Colocalizes with the PKA C Subunit and SC35 in HEK293T Cells—A subpopulation of the PKA C subunit has been shown to be localized to SFCs in the nucleus, where it colocalizes with the splicing factor SC35 (29). Furthermore, SFRS17A and SC35 colocalize in well defined spots (Fig. 4, *A–D*), as also shown previously (36). With the use of our newly developed anti-SFRS17A antibodies combined with anti-C antibodies, we found both SFRS17A and the PKA C subunit to be colocalized and present in SFCs of HEK293T cells (Fig. 4, *E–H*). Overexpressed SFRS17A demonstrated a similar localization pattern (data not shown).

Downloaded from www.jbc.org at University of Washington Health Sciences Libraries, on January 7, 2010

Supplemental Material can be found at:
http://www.jbc.org/content/suppl/2009/10/19/M109.056465.DC1.html

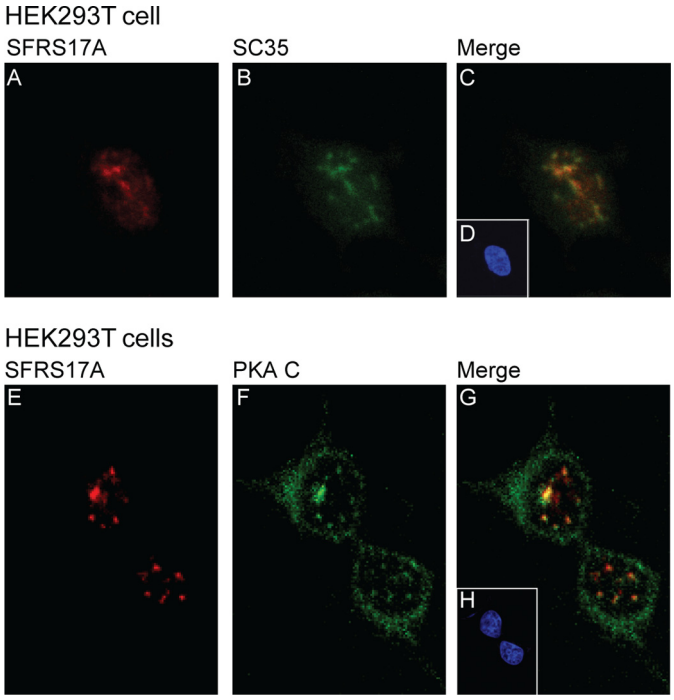

FIGURE 4. **SFRS17A colocalizes with the PKA C subunit and SC35 in HEK293T cells.** *A–D*, immunofluorescence analysis showed colocalization of endogenous SFRS17A and SC35 in HEK293T cells using anti-SFRS17A and anti-SC35. *E–H*, colocalization of endogenous SFRS17A and the PKA C subunit in HEK293T cells was shown by immunofluorescence using anti-SFRS17A and anti-PKA C. Nuclei were stained with DAPI (*D* and *H*). *Merged images* show overlapping subcellular distribution that appears *yellow* (*C* and *G*).

Expression of SFRS17A with an Intact PKA Binding Domain Facilitates Splicing of the E1A Minigene—Introduction of four prolines in the R-binding region 2 of SFRS17A (L438P/L439P/K445P/K446P) abolished binding to PKA RI in a co-immunoprecipitation experiment (Fig. 5*A*). This mutant was further used as a negative control in an *E1A* pre-mRNA splicing experiment. The presence of three alternative 5′ splice sites in the *E1A* pre-mRNA results in three major mRNAs (13, 12, and 9 S) (43). In addition, two minor mRNAs (11 and 10 S) are created by usage of an additional internal 3′ splice site acceptor (44) (schematically illustrated in Fig. 5*B*). In U-2OS cells transfected with *E1A* and empty FLAG-vector, we detected 13 and 12 S mRNAs as the major mRNA products (Fig. 5*D*, *lane 1*), indicating that mRNAs generated by proximal splice site selection are mainly detected in U-2OS cells. Overexpression of T7-ASF/SF2 as a control resulted in elevated levels of the 13 S proximal splice product as expected, with the other mRNA products being essentially absent (Fig. 5*D*, *lane 5*) (45). The splicing analysis indicated that overexpression of SFRS17A-FLAG gives activation of the distal 9 S splice site, resulting in increased levels of 9 S mRNA products compared with the vector control (Fig. 5, *D* and *E*, $p < 0.05$) and decreased levels of the 13 S mRNA product ($p < 0.05$). This indicates that SFRS17A modulates the 5′ splice site selection from proximal to distal sites. Similarly, a shift to distal 5′ splice site selection was also observed in U-2OS cells transfected with PKA-C, as previously reported (29) (Fig. 5, *D* and *E*, $p < 0.05$). In contrast to the significant effect of SFRS17A wild type overexpression on the *E1A* splicing pattern, overexpression of SFRS17A mut only resulted in decreased levels of 13 S and increased levels of 12 S (Fig. 5, *D* and *E*, $p < 0.05$). Comparison of the SFRS17A wild type and mutant showed that the decrease of 13 S and increase of 12 and 10 S mRNA products were significant (Fig. 5*E*, $p < 0.05$). The requirement for the presence of the type I PKA binding site in SFRS17A for the regulatory effect on splicing indicates the involvement of type I PKA in the regulation of pre-mRNA splicing and that anchoring of type I PKA to the SFCs via SFRS17A may increase the efficacy of this process.

DISCUSSION

In this report, we demonstrate that the SFRS17A protein, encoded by the pseudoautosomal gene *XE7*, is a dual-specific AKAP. By peptide array and R overlay, SPR kinetic analysis, immunoprecipitations, solid phase pull-down, and cAMP affinity chromatography, we show that SFRS17A binds both type I and type II PKA. Furthermore, we demonstrate by immunofluorescence analysis that SFRS17A colocalizes with the C subunit of PKA and the splicing factor SC35 in nuclear speckles. Using the *E1A* minigene in a pre-mRNA splicing experiment, we also show that expression of wild type SFRS17A, but not SFRS17A substituted to abolish PKA binding, confers PKA-mediated regulation of pre-mRNA splicing.

Our recent discovery of the RISR, an additional PKA binding region in dual-specificity AKAPs, provided new means to classify this group of AKAPs (27). Furthermore, the RISR provided us with a new tool to explore existing data bases for novel, potential AKAPs by using the RISR-generated sequence as bait in a bioinformatic search. A short list of potential, novel AKAPs was unraveled from the search, among them the splicing factor SFRS17A.

Conventional AKAPs are classified by their ability to co-purify with the PKA holoenzyme from tissues or cell lysates. They typically contain a stretch of 14–18 amino acids forming an amphipathic helix that binds to the R subunit of PKA (16–18). SFRS17A co-purified with the PKA holoenzyme, as evident from immunoprecipitations, cAMP affinity chromatography, and solid phase pull-down and thus meets the criteria for being an AKAP. When performing a peptide array scan through the entire SFRS17A protein sequence, we observed three stretches of spots binding PKA. Following secondary structure prediction, the most N-terminal of the sequences turned out to be a typical amphipathic helix binding both type I and type II PKA, whereas the most C-terminal type I PKA binding sequence was the RISR-like sequence in SFRS17A, which also contained an amphipathic helix.

Alignment of SFRS17A with different AKAPs showed that the RISR of SFRS17A aligned with the PKA binding region of pericentrin both in the forward and the reverse direction (supplemental Fig. S2*B*). Although the 100-amino acid-long PKA binding region in pericentrin is shown only to bind type II PKA through a motif different from the amphipathic helix, it is interesting to speculate whether this long binding region also encompasses a repeated and inverted RISR, with a stretch of amino acids in between that confers RII specificity, possibly by binding to the hydrophobic groove in the D/D domain. The structure of the D/D domain of PKA RI consists of a symmetrically organized X-type antiparallel dimer forming the AKAP

Downloaded from www.jbc.org at University of Washington Health Sciences Libraries, on January 7, 2010

Supplemental Material can be found at:
http://www.jbc.org/content/suppl/2009/10/19/M109.056465.DC1.html

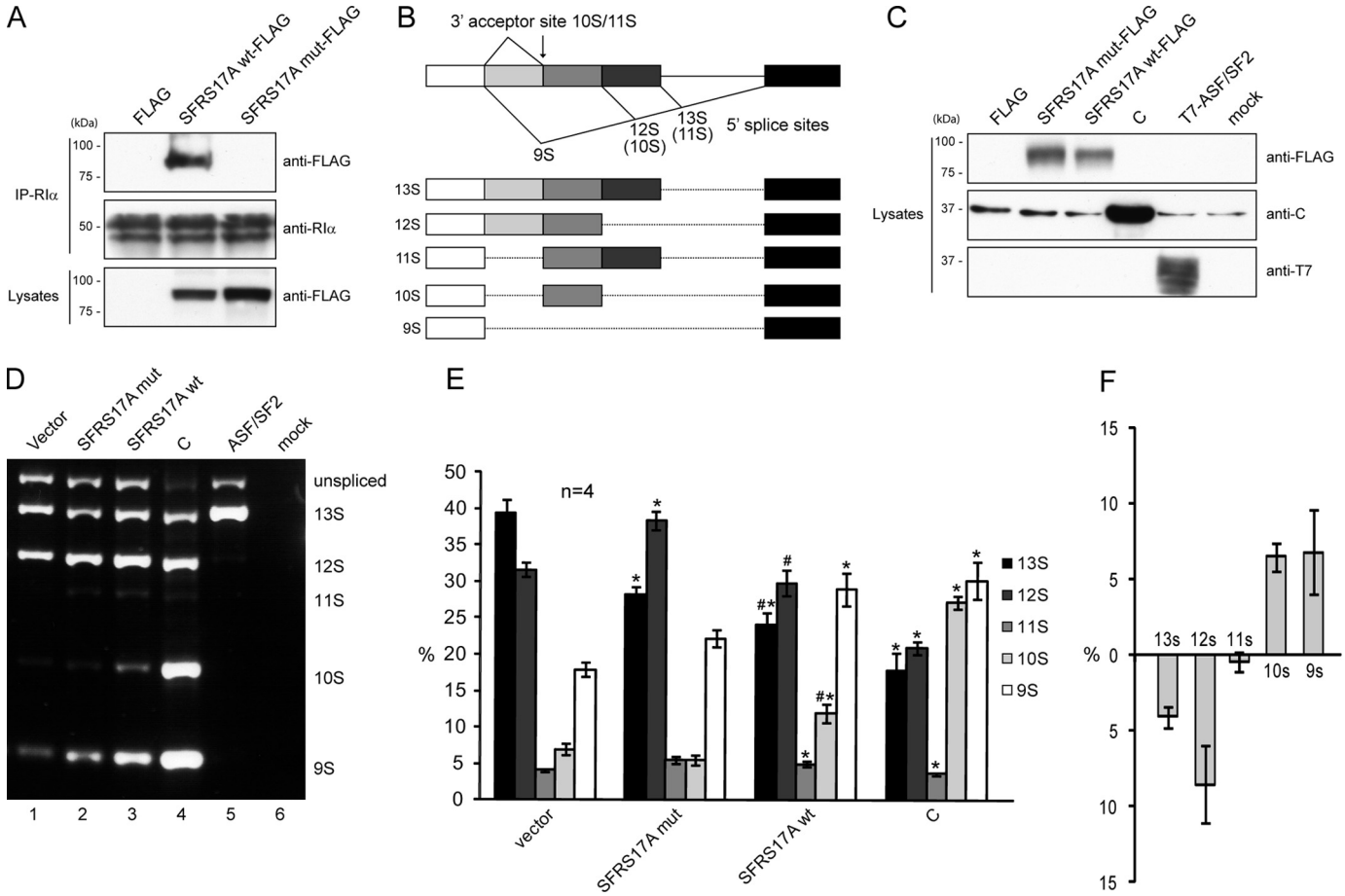

FIGURE 5. **SFRS17A influences *E1A* splicing *in vivo*.** *A*, co-immunoprecipitation (*IP*) of FLAG-SFRS17A wild type (*wt*) protein or FLAG-SFRS17A(L438P/L439P/K445P/K446P) (*SFRS17A mut*) protein with PKA-RIα, as detected by anti-FLAG immunoblotting. The *immunoblot* shown is one of two independent experiments. *B*, schematic presentation of possible alternative splice variants of the *E1A* minigene. *C*, U-2OS cells were transiently cotransfected with 0.5 μg of the splicing reporter minigene *E1A* and 1.5 μg of either Cα, SFRS17A, SFRS17A(L438P/L439P/K445P/K446P), or ASF/SF2. The total amount of DNA used for the transfection was kept constant by adding empty plasmid DNA. Immunoblot was probed with anti-FLAG, anti-C, or anti-T7 to monitor expression levels. *D*, total RNA was extracted from the same samples 20 h after transfection and analyzed by reverse transcription-PCR. The GelStar-stained agarose gel shown is from one representative experiment. *E*, the relative levels of the splice products were analyzed by densitometry (mean ± S.E., $n = 4$); *, $p < 0.05$ compared with control by paired, two-tailed Student's *t* test. #, $p < 0.05$ compared with SFRS17A mutant by paired, two-tailed Student's *t* test. *F*, the relative levels of the splice products for SFRS17Awt *versus* SFRS17Amut (mean +/- S.E., $n = 4$).

binding groove (21). Due to the symmetry axis, the AKAP can bind to both R subunits in the hydrophobic groove of the R dimer in either orientation. This may provide the basis for why the SFRS17A RISR binds PKA when spotted in both directions (Fig. 1*C*) because it can contact either of the two R protomers. Furthermore, this symmetry could be why the RISR aligns with the PKA binding region of pericentrin in both forward and reverse sequence. Real time kinetics studies (SPR) of the SFRS17A-PKA interaction revealed that SFRS17A binds type I and type II PKA with similar affinities in the low nanomolar range. This is in contrast to most AKAPs studied so far because they have been shown to bind RII with higher affinity than RI due to the more dynamic state of the type I PKA·AKAP complex, generally reflected in the dissociation rate, which is ~100-fold higher for RIα than the RIIα subunit (16, 24, 39). This formed the basis for our opinion that SFRS17A is a true dual-specific AKAP, binding equally well to both type I and type II PKA. A plausible explanation for this observation could be that the RISR contributes to the higher affinity for RI by providing multisite contact with the RI subunit that may stabilize the anchored type I PKA complex and thus compensates for the relatively lower affinity and faster off-rate of RI compared with RII binding to the amphipathic helix. We have previously shown that the RISR confers RI specificity to dual-specificity AKAPs, such as Ezrin (27), and this was further confirmed in the SPR studies because a RISR peptide partially disrupted the type I PKA-SFRS17A interaction but not the interaction with type II PKA.

SFRS17A was present in all cell lines tested, as revealed by reverse transcription-PCR, indicating that the protein is ubiquitously expressed in line with what has previously been reported regarding this protein being a housekeeping gene (46). The antibody characterized in this work was able to detect endogenous SFRS17A, which simplifies the characterization of this protein compared with previous reports that have based their conclusions on overexpression of SFRS17A. It also enabled us to do some of our experiments with the endogenous SFRS17A protein.

Proteins involved in pre-mRNA splicing are located in SFCs. It has been demonstrated that overexpressed SFRS17A colocalizes with the splicing factor SC35 in the nucleus (36), and in our study we obtained similar results from co-staining experiments

Downloaded from www.jbc.org at University of Washington Health Sciences Libraries, on January 7, 2010

Supplemental Material can be found at:
http://www.jbc.org/content/suppl/2009/10/19/M109.056465.DC1.html

of endogenous SFRS17A and SC35. In addition, immunofluorescence experiments showed that SFRS17A colocalizes with the C subunit of PKA, placing all three proteins in SFCs. The C subunit was previously shown to be involved in regulation of pre-mRNA splicing (29) along with SFRS17A (36), SC35 (32), and numerous other proteins. Using an *in vivo* splicing assay, we demonstrated that SFRS17A had a significant effect on the alternative splice site selection of the adenoviral *E1A* gene. Furthermore, we also observed a similar splicing pattern for SFRS17A and the C subunit of PKA with increased expression of the two mRNAs of 10 and 9 S, whereas the larger mRNA product, 13 S, was reduced when compared with vector control. These findings indicate that SFRS17A promotes distal 5′ splice site selection. In contrast, introduction of SFRS17A, substituted to abolish type I PKA binding, did not confer the same effect on splicing, although it did appear to have some PKA-independent effect on the splicing pattern. Hence, we concluded that SFRS17A is involved in regulation of pre-mRNA splicing but that type I PKA, anchored through SFRS17A, appears to be necessary for activation of the distal 5′ splice site.

Several models may be envisioned for how PKA can regulate pre-mRNA splicing. The most obvious model would be that PKA affects splicing directly by binding to the AKAP SFRS17A and thereby being positioned to phosphorylate nearby substrates in the splicing factor compartments. It has, in fact, earlier been shown that PKA can phosphorylate the SR protein ASF/SF2 *in vitro* (47) and the polypyrimidine tract-binding protein *in vivo* (48). Studies have, however, been conducted that suggest that pre-mRNA splicing is regulated by PKA through a cAMP-independent mechanism (29). The latter finding implies either that the regulation is mediated by free PKA C subunits or that the PKA R_2C_2 complex would not have to be activated by cAMP and could remain as an intact holoenzyme while regulating this process. Furthermore, PKA may recruit other proteins that have a regulatory role in the pre-mRNA splicing process. However, overexpression of the R subunits alone did not seem to influence the splicing pattern of the *E1A* minigene (data not shown), and further studies are needed to unravel the exact role of PKA in pre-mRNA splicing.

Although it is established that SFRS17A is a nuclear protein, the occurrence of R subunits in the nucleus remains elusive. However, some reports have been made that suggest the identification of R subunits in the nucleus (49–55). The uncertainty in this field may be based on the possibility that a nuclear R subunit is of low abundance and/or may only enter the nucleus when the nuclear envelope is disassembled at mitosis, leaving small pools of PKA associated with distinct AKAPs. Furthermore, we explored the possibility that SFRS17A could bind directly to the C subunit of PKA, but SPR studies, performed with C in the absence of R, did not show any interaction with SFRS17A; nor did C overlay on SFRS17A peptide arrays identify any interaction (data not shown). However, SPR studies performed with the intact PKA holoenzyme did show interaction, indicating that the R subunit is required for the interaction with SFRS17A (data not shown). Another intriguing possibility could be that SFRS17A shuttles in and out of the nucleus like its interaction partner ASF/SF2 (56) and carries PKA as cargo. However, preliminary immunofluorescence experiments using leptomycin B to inhibit active nuclear export and a combination of actinomycin D and cycloheximide to terminate ongoing transcription needed for nuclear reimport have not been able to confirm this. In summary, our data show that SFRS17A is a dual-specificity AKAP that targets PKA to the SFCs to confer PKA regulation of pre-mRNA splicing through a yet unknown mechanism.

Acknowledgments—We are grateful to Jorun Solheim, Gladys M. Tjørhom, and Guri Opsahl for technical assistance, Ola Blingsmo for peptide synthesis, and Sissel Eikvar (Department of Nutrition, University of Oslo) for assistance with the E1A splicing assay.

REFERENCES

1. Jarnaess, E., and Taskén, K. (2007) *Biochem. Soc. Trans.* **35,** 931–937
2. Dell'Acqua, M. L., and Scott, J. D. (1997) *J. Biol. Chem.* **272,** 12881–12884
3. Taylor, S. S., Buechler, J. A., and Yonemoto, W. (1990) *Annu. Rev. Biochem.* **59,** 971–1005
4. Skalhegg, B. S., and Tasken, K. (2000) *Front. Biosci.* **5,** D678–D693
5. Taskén, K., and Aandahl, E. M. (2004) *Physiol. Rev.* **84,** 137–167
6. Wong, W., and Scott, J. D. (2004) *Nat. Rev. Mol. Cell Biol.* **5,** 959–970
7. Angelo, R., and Rubin, C. S. (1998) *J. Biol. Chem.* **273,** 14633–14643
8. Küssel-Andermann, P., El-Amraoui, A., Safieddine, S., Hardelin, J. P., Nouaille, S., Camonis, J., and Petit, C. (2000) *J. Biol. Chem.* **275,** 29654–29659
9. Lim, C. J., Han, J., Yousefi, N., Ma, Y., Amieux, P. S., McKnight, G. S., Taylor, S. S., and Ginsberg, M. H. (2007) *Nat. Cell Biol.* **9,** 415–421
10. Grönholm, M., Vossebein, L., Carlson, C. R., Kuja-Panula, J., Teesalu, T., Alfthan, K., Vaheri, A., Rauvala, H., Herberg, F. W., Taskén, K., and Carpén, O. (2003) *J. Biol. Chem.* **278,** 41167–41172
11. Huang, L. J., Durick, K., Weiner, J. A., Chun, J., and Taylor, S. S. (1997) *J. Biol. Chem.* **272,** 8057–8064
12. Huang, L. J., Durick, K., Weiner, J. A., Chun, J., and Taylor, S. S. (1997) *Proc. Natl. Acad. Sci. U.S.A.* **94,** 11184–11189
13. Li, H., Degenhardt, B., Tobin, D., Yao, Z. X., Tasken, K., and Papadopoulos, V. (2001) *Mol. Endocrinol.* **15,** 2211–2228
14. Reinton, N., Collas, P., Haugen, T. B., Skålhegg, B. S., Hansson, V., Jahnsen, T., and Taskén, K. (2000) *Dev. Biol.* **223,** 194–204
15. Liu, J., Rone, M. B., and Papadopoulos, V. (2006) *J. Biol. Chem.* **281,** 38879–38893
16. Carr, D. W., Stofko-Hahn, R. E., Fraser, I. D., Bishop, S. M., Acott, T. S., Brennan, R. G., and Scott, J. D. (1991) *J. Biol. Chem.* **266,** 14188–14192
17. Hausken, Z. E., Coghlan, V. M., Hastings, C. A., Reimann, E. M., and Scott, J. D. (1994) *J. Biol. Chem.* **269,** 24245–24251
18. Hausken, Z. E., and Scott, J. D. (1996) *Biochem. Soc. Trans.* **24,** 986–991
19. Newlon, M. G., Roy, M., Morikis, D., Hausken, Z. E., Coghlan, V., Scott, J. D., and Jennings, P. A. (1999) *Nat. Struct. Biol.* **6,** 222–227
20. Newlon, M. G., Roy, M., Morikis, D., Carr, D. W., Westphal, R., Scott, J. D., and Jennings, P. A. (2001) *EMBO J.* **20,** 1651–1662
21. Banky, P., Roy, M., Newlon, M. G., Morikis, D., Haste, N. M., Taylor, S. S., and Jennings, P. A. (2003) *J. Mol. Biol.* **330,** 1117–1129
22. Gold, M. G., Lygren, B., Dokurno, P., Hoshi, N., McConnachie, G., Taskén, K., Carlson, C. R., Scott, J. D., and Barford, D. (2006) *Mol. Cell* **24,** 383–395
23. Kinderman, F. S., Kim, C., von Daake, S., Ma, Y., Pham, B. Q., Spraggon, G., Xuong, N. H., Jennings, P. A., and Taylor, S. S. (2006) *Mol. Cell* **24,** 397–408
24. Alto, N. M., Soderling, S. H., Hoshi, N., Langeberg, L. K., Fayos, R., Jennings, P. A., and Scott, J. D. (2003) *Proc. Natl. Acad. Sci. U.S.A.* **100,** 4445–4450
25. Carlson, C. R., Lygren, B., Berge, T., Hoshi, N., Wong, W., Taskén, K., and Scott, J. D. (2006) *J. Biol. Chem.* **281,** 21535–21545
26. Burns-Hamuro, L. L., Ma, Y., Kammerer, S., Reineke, U., Self, C., Cook, C., Olson, G. L., Cantor, C. R., Braun, A., and Taylor, S. S. (2003) *Proc. Natl. Acad. Sci. U.S.A.* **100,** 4072–4077
27. Jarnaess, E., Ruppelt, A., Stokka, A. J., Lygren, B., Scott, J. D., and Taskén,

Downloaded from www.jbc.org at University of Washington Health Sciences Libraries, on January 7, 2010

Supplemental Material can be found at:
http://www.jbc.org/content/suppl/2009/10/19/M109.056465.DC1.html

K. (2008) *J. Biol. Chem.* **283,** 33708–33718
28. Diviani, D., Langeberg, L. K., Doxsey, S. J., and Scott, J. D. (2000) *Curr. Biol.* **10,** 417–420
29. Kvissel, A. K., Ørstavik, S., Eikvar, S., Brede, G., Jahnsen, T., Collas, P., Akusjärvi, G., and Skålhegg, B. S. (2007) *Exp. Cell Res.* **313,** 2795–2809
30. Ge, H., Zuo, P., and Manley, J. L. (1991) *Cell* **66,** 373–382
31. Krainer, A. R., Mayeda, A., Kozak, D., and Binns, G. (1991) *Cell* **66,** 383–394
32. Fu, X. D., and Maniatis, T. (1990) *Nature* **343,** 437–441
33. Lamond, A. I., and Spector, D. L. (2003) *Nat. Rev. Mol. Cell Biol.* **4,** 605–612
34. Wu, J. Y., and Maniatis, T. (1993) *Cell* **75,** 1061–1070
35. Kohtz, J. D., Jamison, S. F., Will, C. L., Zuo, P., Lührmann, R., Garcia-Blanco, M. A., and Manley, J. L. (1994) *Nature* **368,** 119–124
36. Mangs, A. H., Speirs, H. J., Goy, C., Adams, D. J., Markus, M. A., and Morris, B. J. (2006) *Nucleic Acids Res.* **34,** 4976–4986
37. Ellison, J. W., Ramos, C., Yen, P. H., and Shapiro, L. J. (1992) *Hum. Mol. Genet.* **1,** 691–696
38. Hillman, R. T., Green, R. E., and Brenner, S. E. (2004) *Genome Biol.* **5,** R8
39. Herberg, F. W., Maleszka, A., Eide, T., Vossebein, L., and Tasken, K. (2000) *J. Mol. Biol.* **298,** 329–339
40. Frank, R. (2002) *J. Immunol. Methods* **267,** 13–26
41. Hausken, Z. E., Coghlan, V. M., and Scott, J. D. (1998) *Methods Mol. Biol.* **88,** 47–64
42. Durgerian, S., and Taylor, S. S. (1989) *J. Biol. Chem.* **264,** 9807–9813
43. Cáceres, J. F., Stamm, S., Helfman, D. M., and Krainer, A. R. (1994) *Science* **265,** 1706–1709
44. Ulfendahl, P. J., Linder, S., Kreivi, J. P., Nordqvist, K., Sevensson, C., Hultberg, H., and Akusjärvi, G. (1987) *EMBO J.* **6,** 2037–2044
45. Krainer, A. R., Conway, G. C., and Kozak, D. (1990) *Cell* **62,** 35–42
46. Lau, Y. F., and Zhang, J. (2000) *Mol. Carcinog.* **27,** 308–321
47. Colwill, K., Pawson, T., Andrews, B., Prasad, J., Manley, J. L., Bell, J. C., and Duncan, P. I. (1996) *EMBO J.* **15,** 265–275
48. Xie, J., Lee, J. A., Kress, T. L., Mowry, K. L., and Black, D. L. (2003) *Proc. Natl. Acad. Sci. U.S.A.* **100,** 8776–8781
49. Cumming, R., Koide, Y., Krigman, M. R., Beavo, J. A., and Steiner, A. L. (1981) *Neuroscience* **6,** 953–961
50. Fletcher, W. H., Van Patten, S. M., Cheng, H. C., and Walsh, D. A. (1986) *J. Biol. Chem.* **261,** 5504–5513
51. Kuettel, M. R., Squinto, S. P., Kwast-Welfeld, J., Schwoch, G., Schweppe, J. S., and Jungmann, R. A. (1985) *J. Cell Biol.* **101,** 965–975
52. Vuong, B. Q., Lee, M., Kabir, S., Irimia, C., Macchiarulo, S., McKnight, G. S., and Chaudhuri, J. (2009) *Nat. Immunol.* **10,** 420–426
53. Gupte, R. S., Sampson, V., Traganos, F., Darzynkiewicz, Z., and Lee, M. Y. (2006) *Exp. Cell Res.* **312,** 796–806
54. Gupte, R. S., Weng, Y., Liu, L., and Lee, M. Y. (2005) *Cell Cycle* **4,** 323–329
55. Gupte, R. S., Pozarowski, P., Grabarek, J., Traganos, F., Darzynkiewicz, Z., and Lee, M. Y. (2005) *Cancer Biol. Ther.* **4,** 429–437
56. Cáceres, J. F., Screaton, G. R., and Krainer, A. R. (1998) *Genes Dev.* **12,** 55–66

Downloaded from www.jbc.org at University of Washington Health Sciences Libraries, on January 7, 2010